Radiation counter tube

Wiedemair Wolfgang
Tscharnuter Daniel

Tutor: Callegari Carlo, PhD.
Date: 9.5.2003

Contents

1 Basics

1.1 Radioactivity

Radioactivity is the emission of radiation from unstable atomic nuclei that was discovered in 1896 by Henri Becquerel. He also proved that this radiation could be deflected by a magnetic field and therefore must consist also of charged particles. In 1903, he was awarded the Nobel Prize for physics together with Pierre and Marie Curie.
The radiation is emitted in the form of a positively charged alpha particle (a helium nucleus), a beta particle (either an electron or positron), or gamma rays. Nuclear fission is also a radioactive process, where elements become unstable after absorbing a neutron. Common radioactive isotopes are uranium 235 and plutonium 239. They are used in nuclear reactors and nuclear weapons. A splitting nucleus releases energy by radiation, emission of neutrons and also smaller nuclei.

1.1.1 α-decay

α-decay is the emission of an alpha particle ($^4_2$He nucleus). An example of this is the decay of uranium:

$$^{238}_{92}\mathrm{U} \longrightarrow {}^{234}_{90}\mathrm{Th} + {}^{4}_{2}\mathrm{He}$$

Alpha particles are the least penetrating of the particles produced in a radioactive decay because of their large mass and their charge of $+2e$.

1.1.2 β decay

β decay is the emission of a beta particle, which can be either an electron or a positron. A positron is the antiparticle of the $+e$. The β decay was explained as the decay of a particle in the nucleus, e.g.

$$\mathrm{n} \longrightarrow \mathrm{p} + \mathrm{e}^-$$

In experiments it was observed that this decay breaks the law of the conservation of energy and momentun. In 1930, Pauli postulated a new particle to save the conservation laws. He called the new particle neutron, but it was later given the name neutrino (*"little neutron"* by Fermi.
The existence of neutrinos has been experimentally proven[1]. Because of the conservation laws of spin and charge, neutrinos have no charge and spin is $\frac{1}{2}$. The neutrino mass is very small (estimates less than 3eV[2]).

A well known example of β-decay is the decay of carbon to nitrogen:

$$^{14}_{6}\mathrm{C} \longrightarrow {}^{14}_{7}\mathrm{N} + \mathrm{e}^{-} + \nu$$

Beta particles are more penetrating than alpha particles.

1.1.3 γ-decay

γ-decay is the emission of high energy photons. γ-decay occurs when a nucleus is left in an excited state after an alpha or beta decay[3]. After a β-decay of caesium to barium (the $'$ indicates an excited state of the nucleus)

$$^{137}_{55}\mathrm{Cs} \longrightarrow {}^{137}_{56}\mathrm{Ba}' + \mathrm{e}^{-} + \nu$$

the barium undergoes γ decay to

$$^{137}_{56}\mathrm{Ba}' \longrightarrow {}^{137}_{56}\mathrm{Ba} + \gamma$$

γ rays are highly penetrating, with sufficient energy they can penetrate a couple of centimeters of lead.

1.2 Radiation counters

A radiation counter is a device to detect and measure the amount of ionizing radiation (α, β, γ radiation). In principle, all types of radiation detectors detect the ions and electrons produced when the ionizing radiation interacts with matter. A few different types of radiation detectors are

- Ionization chambers
- Gas filled counter tubes
- Semiconductor detectors
- Scintillation counters
- Fog chambers

[2]http://www.nobel.se/physics/laureates/2002/public.html
[2]http://www.physik.uni-mainz.de/exakt/neutrino/en_index.html
[3]E.W. Schpolski, Atomphysik Bd. II

In our experiments, we will use gas-filled radiation counter tubes. This type of detectors consist of a conducting tube with a thin wire in its center. A voltage U is applied between the wire and the tube. The wire needs to be thin to achieve high electric field strengths in the surrounding of the wire.
When an ionizing particle enters the tube, it will ionize a number of gas atoms, one speaks of primary ionization.

1.2.1 Proportional counter

The proportional counter is a gas-filled tube counter. In order to detect a single particle, a large number of ions is required. The voltage U is chosen so that, when an ionizing particle causes ionizations, the released electrons don't recombine with the gas ions. The electrons are accelerated in the electric field and can acquire enough energy to again cause ionization of gas atoms. Additionally, gas atoms can be excited by the electrons and emit photons, which can cause photoinization. Because of these ionization processes the gas amplifies the charge from the primary ionization by a factor of up to 10^5. The voltage U is high enough so that the released electrons are quickly collected at the wire, so there is a sudden increase of charge at the wire. This charge pulse corresponds to the series of ionizations caused by an ionizing particle entering the tube. The amount of charge in a pulse is proportional to the ionizing charge.
A proportional counter is works at a linear relation between the voltage and the energy of the detected particle.

1.2.2 Geiger-Müller counter

The Geiger-Müller counter is basically a proportional counter that works at a higher voltage U. Geiger-Müller counters produce larger pulses than other types of detectors. The main difference between the proportional couter and the Geiger-Müller counter is that *the number of collected electrons does not depend on the applied voltage nor on the number of electrons produced by the initial radiation.*

When a particle has been detected by the released electrons, positive ions remain. Because of their large mass these ions move slowly compared to the electrons, this is why they form a positive charge cloud (*space charge*) around the wire. However the positive ions do not increase the electric field of the positive wire but act like a thicker wire and thus lower the field strength. This prevents further secondary ionization. The ions drift to the negative chamber wall and are neutralised there. In doing so they can free electrons from the chamber wall. These electrons would cause further ionizations and thus lead to a chain reaction. There are two different approaches to prevent this chain reaction:

- The applied voltage is turned off or inverted.
- An organic *quenching gas* is used to prevent further ionization.

1.2.3 Characteristic curve of the counter

The count rate can be determined as a function of the applied voltage. The characteristic curve is the plot of the count rate z and the voltage U. The curve is divided into regions

such as the proportional area and the Geiger-Müller region.
An incoming particle creates about 10^4 gas ions (depending on its energy). This number does not depend on the voltage. When there is no voltage applied, the electrons and the ions recombine and no pulse will be measured. With increasing voltage a number of electrons reach the wire and produce a signal. At a certain voltage all electrons reach the wire, this is where the first plateau begins. On this plateau, the count rate is practically independent of the voltage. The quality of the counter can be expressed in terms of the slope of this plateau:

$$p = \frac{z_2 - z_1}{z} * 100 \quad \frac{\%}{100V}$$

1.2.4 Correction of the count rate

If n particles are counted during the period of time Δt, the count rate is

$$z = \frac{n}{\Delta t}$$

The time resolution of the counter is limited by the electronics used to register the pulses. The time between two pulses must be at least the *resolution time* τ_A in order to register both pulses. For the count rate this means that the period of time for the n counts was not Δt but $\Delta t - n\tau_A$ instead. The actual count rate is

$$z_w = \frac{n}{\Delta t - n\tau_A}$$

While the wire in the tube is surrounded by positive gas ions, there are no secondary ionizations, which means that a pulse can't be generated by an incoming particle. The counter is insensitve. The ions drift away from the wire and beyond a certain distance, the field strength is again high enough for secondary ionizations. The time the ions take to reach that distance is called the dead time τ_D.
Because the resolution time τ_D can't be measured, the dead time τ_D is used as an approximation.

$$z_w = \frac{n}{\Delta t - n\tau_D}$$

1.3 Energy distribution of the β radiation

A particle with a charge e moving in a magnetic field experiences the Lorentz force

$$\vec{F}_L = e(\vec{v} \times \vec{B})$$

According to the definition of force, the change of the momentum is

$$F = \frac{dp}{dt} = p\frac{v}{r}$$

For a particle moving perpendicular to the magnetic field one gets

$$r = \frac{p}{eB} \tag{1}$$

From eq. 1 we see that if the magnetic field is constant, the radius of curvature r of the trajectory is proportional to the momentum of the particle. If the radius of curvature is kept constant, particles with a certain momentum can be filtered by establishing the required magnetic field strength.
Since β particles move at velocities near the speed of light, relativistic effects must be taken into account.

$$E_k = m_0c^2\left[\sqrt{\frac{p}{m_0c}^2 + 1} - 1\right] = \sqrt{p^2c^2 - m_0^2c^4} - m_0c^2$$

$$v = \frac{c^2p}{E_k + m_0c^2}$$

m_0 ... electron mass $m_0 = 9,109534 \cdot 10^{-31}kg$
e ... elementary charge $e = 1,6021892 \cdot 10^{-9}C$
c ... speed of light $c = 2,99792458 \cdot 10^{8}m/s$

1.4 Absorption of radiation in aluminium

The radioactive source emits β- and γ-radiation. The γ-photons can penetrate the aluminium and therefore don't influence the observed absorption behaviour, they are constantly counted. Along with the background radiation the γ radiation was subtracted from the total count rate.
There are multiple effects that occur when β radiation passes matter:

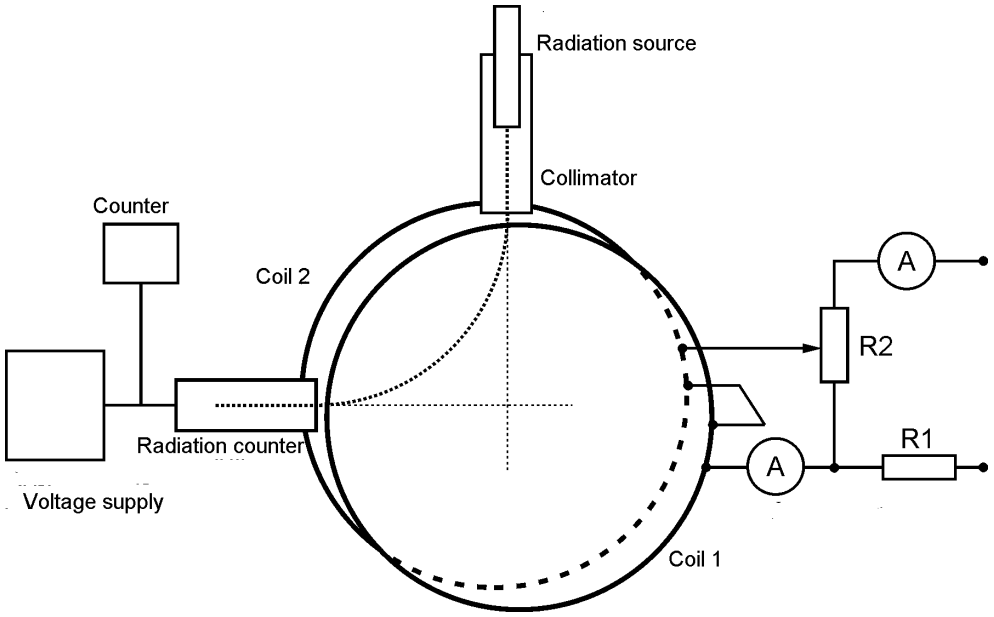

Figure 1: Set-up with magnetic coils as an energy filter for β radiation.

1. Elastic scattering with atom's electrons and nuclei.
2. Ionization of atoms
3. Emission of radiation by deceleration in the electric field of the nuclei (*Bremsstrahlung*).

The combination of these effects is reflected in an **e**mpirical exponential law to describe the absorption.

$$N(d) = N_0\, e^{\mu \cdot d} \tag{2}$$

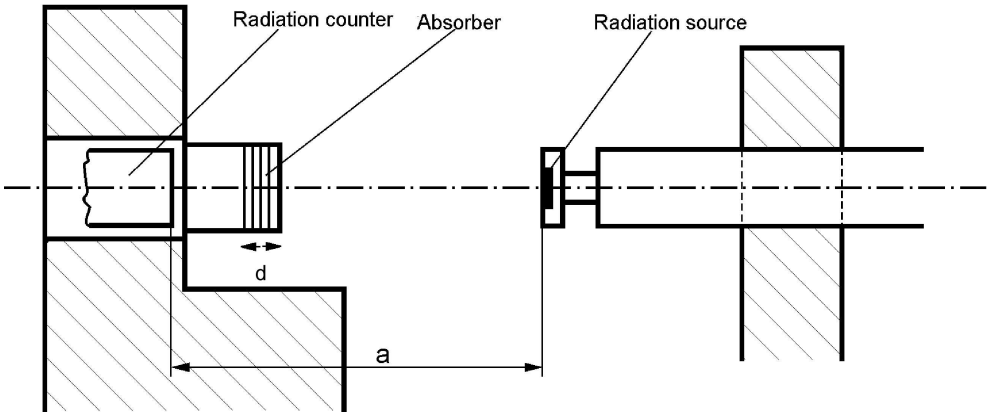

Figure 2: Setup for measuring the absorption of β radiation.

2 Tasks

1. Measure the statistic distribution of the registered impulses.
2. Measure the characteristic curve of the counter.
3. Measure the dead time of the counter.
4. Measure the energy distribution and maximum energy of β-particles.
   - Adjust the source and the counter for momentum filtering with a magnetic field.
   - Measure the count rate for β, γ and the background radiation.
   - Measure the count rate for the γ and the background radiation.
   - Calculate the maximum energy of the β-particles.
5. Measure the absorption of β-particles in aluminium
   - Measure the count rate of the radiation (includes γ and β radiation) for different absorber widths.
   - Calculate the absorption coefficient μ.

3 Equipment

- radiation counter tube Philips 18504)
  window: Mica ($0.9mm; \rho = 2 - 3mg/(cm^2)$)
  cathode: inner diameter 14.4 mm, length 40 mm
  material: 28 % Cr, 27 % Fe
  filling gas: Ne, Ar, Halogen
  dead time: approx. 100 μ s
  capacity: approx. 2 pF

- Radium radioactive source: $^{226}_{88}$ Ra ; activity: 9 μC; emits α, β, γ - radiation
- Impulse counter Ivatsu SC-7201 VII/1493
- Digital multimeter Mastech M 3900
- Magnetic coils VII/1492
- Collimator
- Gauss-/Teslameter F.W. Bell Model 4048 VII/1494
- Oszilloscope Advance Instruments OS 250
- Aluminium disks

4 Experiments

4.1 Statistical distribution of the registered impulses

The radioactive source and the radiation counter were arranged so that about 1000 impulses per second are recorded. The impulse counter was set to count at intervals of 1s, and for a duration of some minutes the number of registered pulses was recorded. The numbers ranged between 945 and 1050. Most of our measurements were done at the same voltage U, so unless otherwise indicated, the voltage U is 500V.
The underlying distribution is a *Poisson* distribution, which can be approximated by a Gauss distribution for large z.

4.2 Characteristic curve of the radiation counter

The characteristic curve was measured with the same setup as used in the previous experiment. The counting interval was set to 10 seconds and the count rate was measured at various voltages with three measurements at each voltage. This was necessary because of the statistic distribution of the count rate.
After a particle is detected, the output voltage of the counter decreases exponentially. A RC-circuit is used to differentiate the signal voltage. The derivative of the signal on the oscilloscope has the shape of a pulse.
The initial pulse and further, quickly changing pulses were visible on the screen. The time resolution was set to 20μs and the dead time was estimated at voltages between 400V and 600V.

4.3 Energy distribution and maximum energy of β-particles

The equipment was set up as shown in fig.1. Two series of measurements were conducted. In the first series, the magnetic field diverted the β-particles away from the radiation counter. This allowed us to measure the contribution of γ-radiation and background radition. In the second series, the magnetic field's direction was inverted to measure both γ and background radition, and the β-radiation.
A quantum-mechanical treatment of the decay in perturbation theory gives Fermi's Golden Rule for the total decay rate W_{fi}

$$W_{fi} = \frac{2\pi}{\hbar^2}|H_{fi}|^2\,\rho \qquad \text{where H is the Hamiltonian and } \rho \text{ the density of states.} \tag{3}$$

For the decay rate one gets

$$z(p) = dW_{fi} \propto p^2(E_0 - E_k)^2\,F(Z^{'},E)dp$$

(using the plane wave approximation). F(Z$^{'}$,E) is the Fermi function.

$$F(Z^{'},E) \approx \frac{2\pi\eta}{1-\exp -2\pi\eta} \qquad \text{with} \qquad \eta = -\frac{Z^{'}\alpha}{p/E} \tag{4}$$

From eq.1 one gets

$$\frac{dp}{p} \propto \frac{dr}{r}$$

Thus the decay rate is

$$z(p) = dW_{fi} \propto p^3 (E_0 - E_k)^2 \, F(Z^{'}, E) dp$$

For evaluation purposes one plots $\frac{\sqrt{z}}{\sqrt{p^3 \, F(Z^{'},E)}}$ over E_k, which will give a straight line. This is the so-called Kurie plot. Most of the β decays in the Uranium-Radium series involve Lead, Bismuth, Thallium and Polonium[4]. We used $Z^{'} = 83$ as approximation for the different atomic numbers.
The semilogarithmic plot (fig. 6) of the energy distribution shows two peaks, so there are contributions from two different decay processes. Due to this fact two linear fits were necessary to distinguish the two radioactive sources and to get a reasonable value for the maximum energy.

4.4 Absorption of radiation in Aluminium

A number of aluminium disks with widths ranging from approx. 0.05mm to 1mm where fixed in front of the window of the radiation counter. The source was set up so that we counted approx. 1000 impulses per second without any absorber. We conducted more measurements at small absorber widths than at larger ones because of the higher slope of the absorption curve in this area. Additionaly we expected to see contributions from two different decay processes as in the energy distribution measurement, so, in contrary to the assumptions in the basics, a biexponential decay is assumed for the absorption function. A logarithmic plot including two straight lines is shown in fig.8 to illustrate the two radiators.

[4] see appendix.

5 Results

5.1 Statistical distribution of the registered impulses

The histogram and the Gauss fit were created with Matlab and Origin.

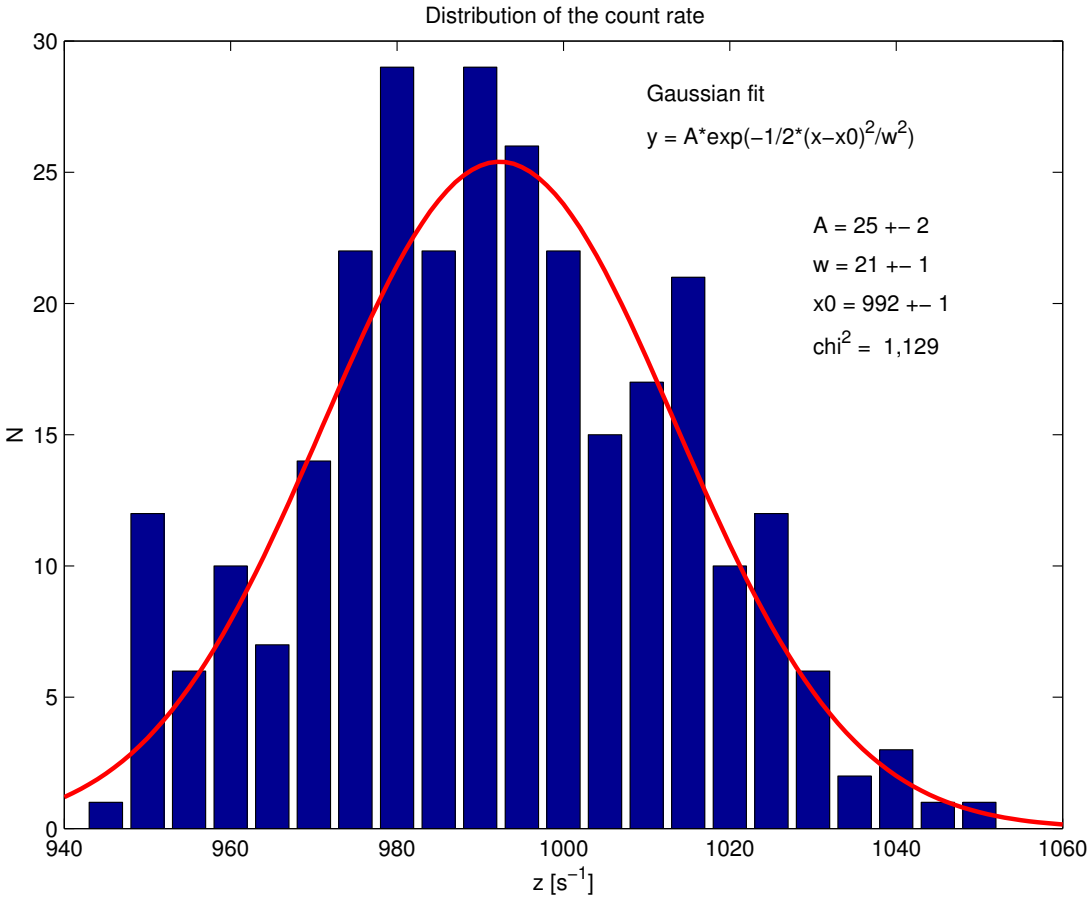

Figure 3: Statistic distribution of the count rate.

5.2 Dead time of the radiation counter

The dead time at 500V which was used in the further experiments is marked bold.
All count rates that were used for calculations are corrected for the dead time.

Table 5.2: **Measurement of the dead time**
Nr.: Number of the measurement
U: Applied voltage
t_{sd}: scale divisions on the oscilloscope, scale of 20μs
τ_D: dead time in μs

Nr.	U/V	t_{sd}/sd	$\tau_D/\mu s$
1	375	8,2	164
2	400	8,4	168
3	425	8,6	172
4	450	8,2	164
5	475	7,8	156
6	**500**	**7,0**	**140**
7	525	6,5	130
8	550	6,0	120
9	575	5,6	112
10	600	5,2	104

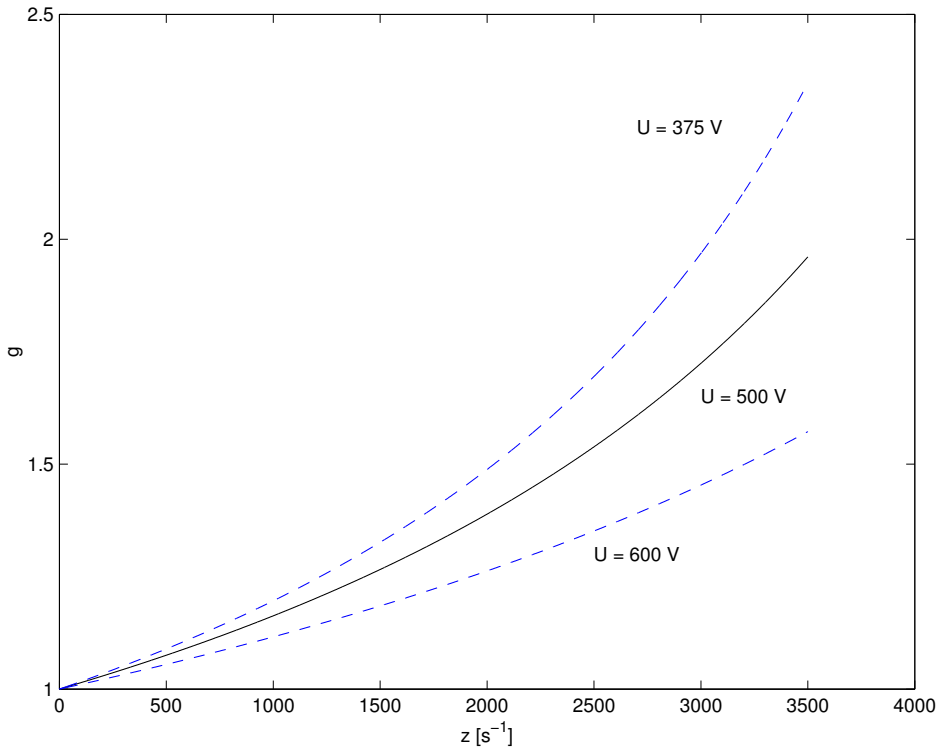

Figure 4: Correction factor g at different voltages.

5.3 Characteristic curve of the radiation counter

Table of results and linear fit for the plateau area:

Table 5.3: **Characteristic curve**
Nr.: Number of the measurement
U: Applied voltage
z_i: measured count rate
z_w: average and dead time corrected count rate
Δz_w: statistical error of z_w

Nr.	U/V	z_1/s^{-1}	z_2/s^{-1}	z_3/s^{-1}	z_w/s^{-1}	$\Delta z_w/s^{-1}$
1	349	3,1	5,8	6,9	5	1
2	350	14,9	13,3	17,0	15	1
3	351	59,6	82,7	50,0	65	3
4	352	111,0	101,6	92,7	103	3
5	355	348,8	561,2	355,8	448	7
6	357	568,9	518,4	529,1	583	8
7	359	791,1	798,8	827,6	908	10
8	361	1091,1	1051,4	1078,9	1264	12
9	363	1162,6	1195,4	1193,5	1419	13
10	365	1023,2	1224,7	1207,7	1373	12
11	375	1229,9	1233,3	1230,1	1487	13
12	370	1208,5	1217,6	1211,8	1461	13
13	380	1179,5	1172,9	1178,9	1409	13
14	390	1124,2	1144,2	1133,0	1348	12
15	400	1116,3	1099,5	1077,1	1297	12
16	410	1065,2	1077,4	1073,8	1261	12
17	420	1058,7	1067,1	1056,2	1246	12
18	430	1033,4	1034,2	1041,0	1212	12
19	440	1039,8	1030,4	1054,6	1219	12
20	450	1027,3	1025,0	1038,0	1204	12
21	460	1004,7	1025,2	1031,7	1191	12
22	470	1019,6	1012,6	1006,2	1180	11
23	480	1009,3	1002,1	1013,2	1174	11
24	490	997,5	992,3	987,9	1153	11
25	500	995,9	1008,7	1000,5	1165	11
26	510	987,5	984,7	993,2	1147	11
27	520	995,4	988,9	984,0	1149	11
28	530	971,6	983,4	979,7	1133	11
29	540	991,0	981,6	977,4	1140	11
30	550	971,3	977,8	975,0	1129	11
31	560	973,0	969,8	988,6	1132	11
32	570	976,8	977,1	971,3	1129	11
33	580	958,2	952,5	997,8	1122	11
34	590	971,6	964,5	967,6	1120	11
35	600	964,2	978,1	962,4	1120	11

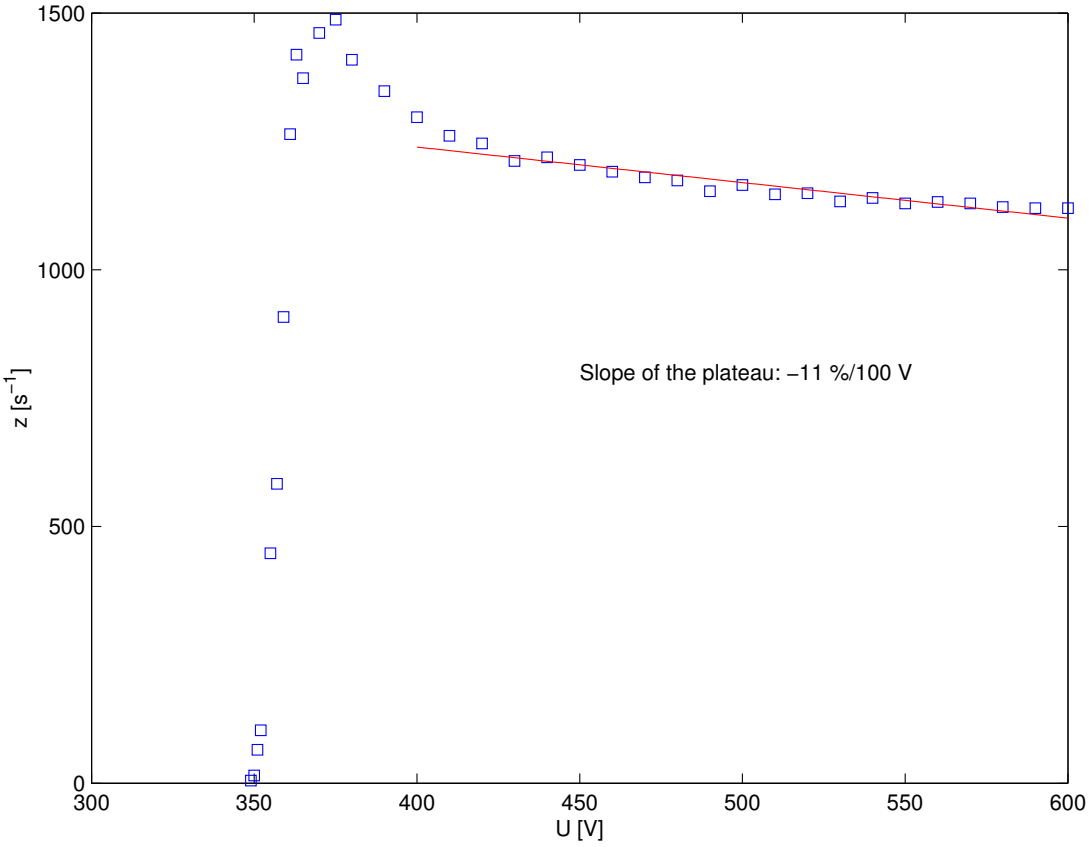

Figure 5: Characteristic curve of the radiation counter. Note that error bars were not included because they were not distinguishable from the markers.

5.4 Energy distribution and maximum energy of β-particles

5.4.1 Data for the γ and background radiation

Table 5.4.1: **Measurement of the γ and background radiation**
Nr.: Number of the measurement
B: Magnetic flux density
z_i: count rate

Nr.	B/mT	z_1/s^{-1}	z_2/s^{-1}
1	2,82	9,23	7,89
2	10,00	8,76	6,15
3	20,40	7,94	10,13
4	30,00	8,64	8,42
5	40,00	8,53	8,56
6	50,10	8,15	8,52
7	60,10	10,22	9,09
8	70,00	9,38	8,10
9	80,00	9,01	10,63
10	90,00	9,23	8,55
11	100,00	7,53	8,85
12	110,00	8,87	9,43
13	120,00	9,34	9,56
14	130,00	8,70	8,07
15	140,00	7,97	9,45
16	150,00	8,69	9,17
17	160,00	8,64	10,22
18	170,00	8,91	9,17
19	180,00	8,03	8,50
20	190,00	7,90	8,28
21	200,00	8,61	7,36
22	210,00	9,19	9,05
23	220,00	9,27	8,85
24	230,00	7,43	8,08
25	240,00	8,93	9,29
26	250,00	7,74	8,88
27	260,00	8,66	8,13
28	270,00	9,04	7,83

The dead time-corrected, average value for the γ and background radiation $z_{\gamma+N}$ is $(8.7 \pm 0.9)s^{-1}$. This value will be subtracted from the count rate for the total radiation to determine the count rate for β particles.

5.4.2 Data for the β, γ and background radiation

Table 5.4.2: **Measurement of the β, γ and background radiation**
Nr.: Number of the measurement
B: Magnetic flux density
z_i: count rate
z_w: dead time corrected, average count rate
Δz_w: statistical error
v: velocity of the β-particles
E: kinetic energy of the β-particles

Nr.	B/mT	z_1/s^{-1}	z_2/s^{-1}	z_w/s^{-1}	$\Delta z_w/s^{-1}$	$\frac{v}{c}$	E/keV
1	2,82	8,71	9,04	9	1	5,6	0,8
2	10,00	8,59	7,95	8	1	19,5	10,0
3	20,40	7,78	8,62	8	1	37,6	40,5
4	30,00	10,12	8,99	10	1	51,2	84,0
5	40,00	9,81	11,11	10	1	62,3	142,0
6	50,10	11,42	12,39	12	1	70,6	210,3
7	60,10	13,48	14,40	14	1	76,7	285,3
8	70,00	16,50	16,11	16	1	81,2	364,9
9	80,00	16,39	14,60	16	1	84,7	449,2
10	90,00	15,81	16,37	16	1	87,3	536,7
11	100,00	15,81	16,87	16	1	89,3	626,5
12	110,00	16,27	17,19	17	1	90,9	718,1
13	120,00	14,83	15,65	15	1	92,2	811,2
14	130,00	14,16	15,06	15	1	93,3	905,5
15	140,00	14,37	12,60	14	1	94,1	1000,8
16	150,00	12,70	11,86	12	1	94,8	1096,8
17	160,00	10,56	12,13	11	1	95,4	1193,4
18	170,00	10,79	9,90	10	1	95,9	1290,6
19	180,00	11,25	10,40	11	1	96,3	1388,3
20	190,00	11,11	11,86	12	1	96,7	1486,4
21	200,00	10,12	12,57	11	1	97,0	1584,8
22	210,00	9,81	13,31	12	1	97,3	1683,5
23	220,00	11,83	10,76	11	1	97,5	1782,5
24	230,00	10,68	10,57	11	1	97,7	1881,7
25	240,00	10,11	11,05	11	1	97,9	1981,0
26	250,00	11,52	10,92	11	1	98,0	2080,6
27	260,00	9,91	10,93	10	1	98,2	2180,3
28	270,00	10,64	9,50	10	1	98,3	2280,1

As the energy distribution indicates, two radiating materials have been observed in the measurement. Therefor two linear fits were performed in the Kurie plot. The maximum energy of the β particles was extrapolated from the fit and is $E_{max} = (3127 \pm 133)keV$, this corresponds to a particle moving at approx. 99% of the speed of light.

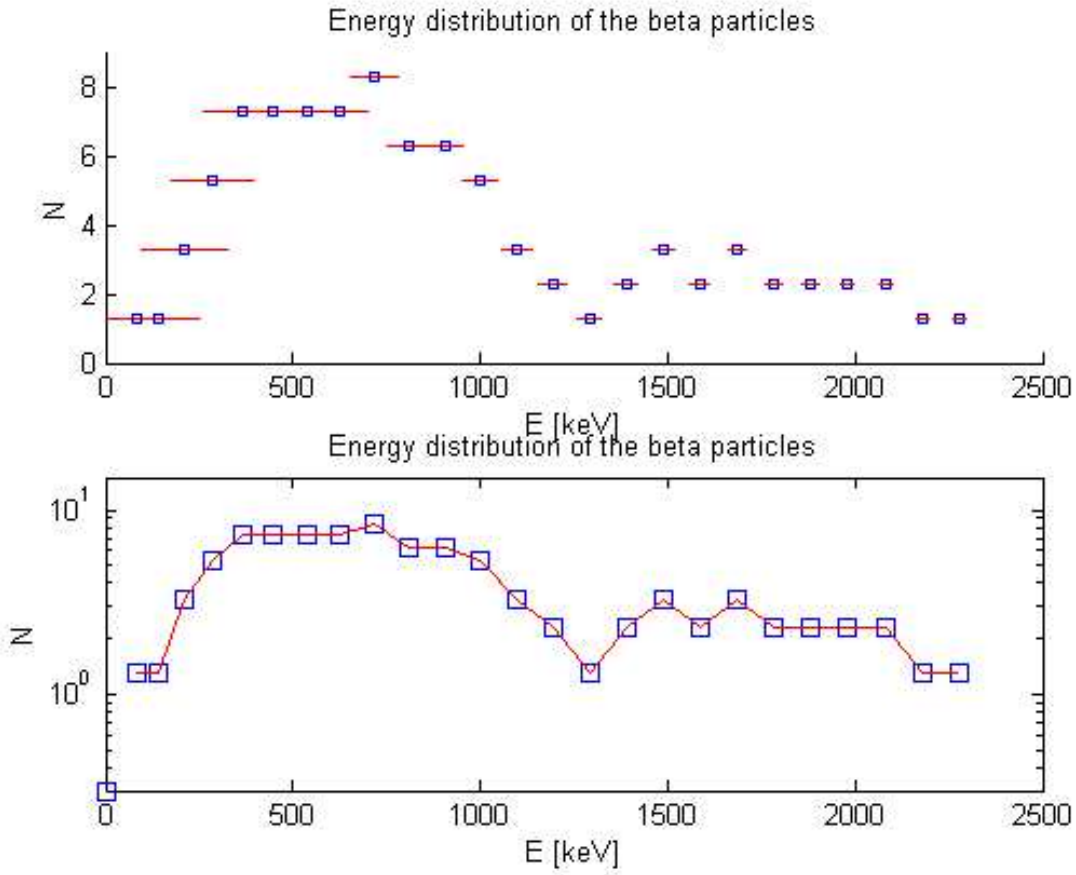

Figure 6: Energy distribution for the β radiation.

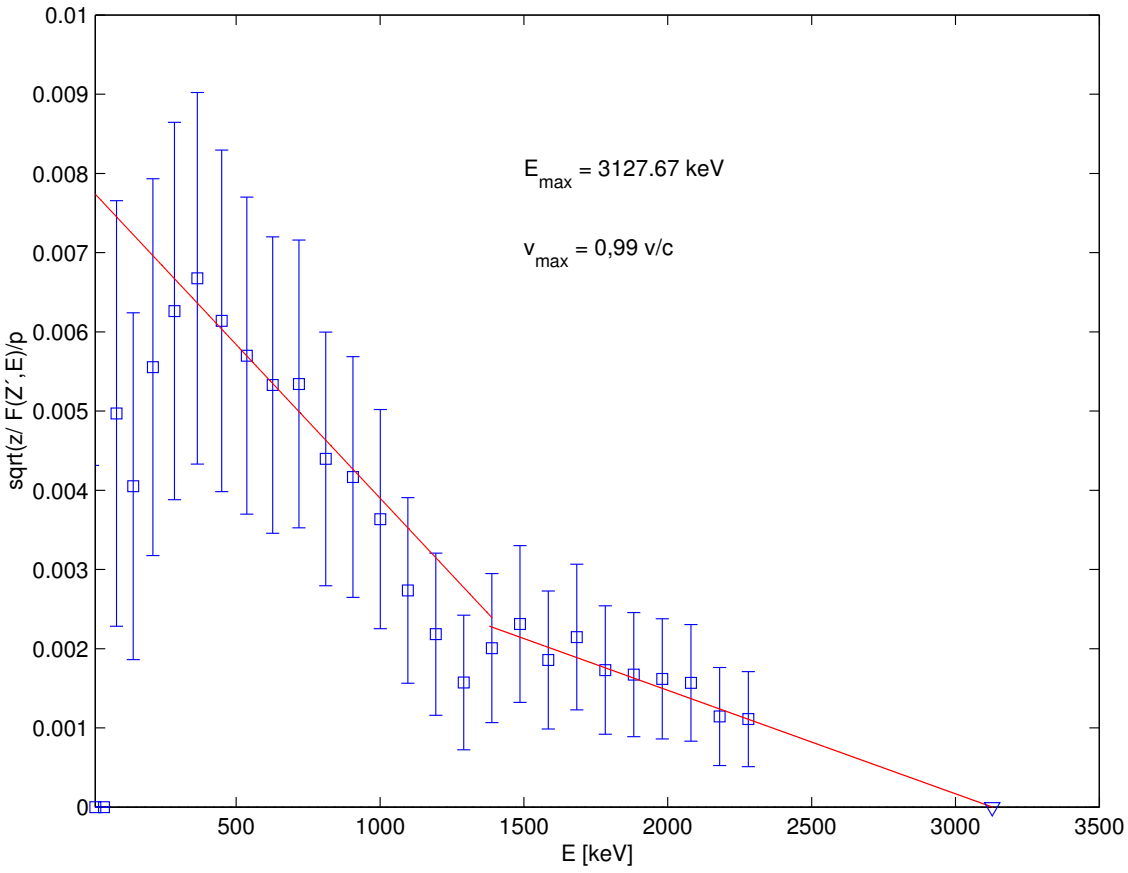

Figure 7: Kurie plot for the β radiation.

5.5 Absorption of radiation in Aluminium

Table 5.5: **Measurement of the absorption in Aluminium**
d: Absorber width
z_i: count rate
z_w: average corrected count rate

Nr.	d/mm	z_1/s^{-1}	z_2/s^{-1}	z_3/s^{-1}	z_w/s^{-1}
1	0,000	1004,9	1025,6	1010,3	1172,5
2	0,055	677,2	673,9	660,6	731,3
3	0,055	678,0	678,8	677,3	740,4
4	0,060	673,6	666,5	661,1	727,1
5	0,060	676,0	676,8	658,3	731,1
6	0,060	669,2	669,5	685,7	736,5
7	0,110	479,9	482,6	493,0	511,8
8	0,110	526,2	517,8	524,2	555,3
9	0,115	481,3	485,7	484,6	510,3
10	0,115	481,6	489,4	475,7	508,4
11	0,120	486,8	493,6	497,5	520,4
12	0,120	491,9	491,6	508,0	525,7
13	0,120	482,1	481,9	483,0	508,6
14	0,120	514,3	516,5	524,1	550,2
15	0,180	414,9	404,2	403,4	423,5
16	0,240	330,8	331,9	323,2	335,8
17	0,300	284,3	282,2	277,2	284,1
18	0,345	241,0	243,6	241,2	241,7
19	0,405	213,0	205,3	222,2	211,4
20	0,460	182,6	188,7	187,1	182,4
21	0,580	148,7	149,6	147,1	142,9
22	0,700	122,4	120,7	125,9	116,5
23	0,820	101,4	101,3	99,9	93,6
24	0,995	74,5	77,2	75,4	67,8
25	1,470	46,8	48,2	50,1	40,0
26	2,000	34,2	33,4	33,6	25,2
27	2,510	28,0	33,2	34,1	23,2
28	3,050	26,8	25,2	24,8	17,0
29	4,110	25,2	24,1	23,7	15,7
30	5,150	20,9	20,6	22,2	12,6
31	6,180	18,5	20,7	21,5	11,6
32	7,250	19,3	20,9	19,2	11,2
33	8,320	18,6	20,9	21,0	11,5
34	8,440	19,9	21,2	19,4	11,5
35	8,560	19,9	20,9	17,7	10,9
36	8,700	21,3	18,3	19,4	11,0
37	8,820	20,9	22,0	19,8	12,3
38	8,930	20,8	17,3	20,1	10,8
39	9,040	20,2	18,5	23,2	12,0

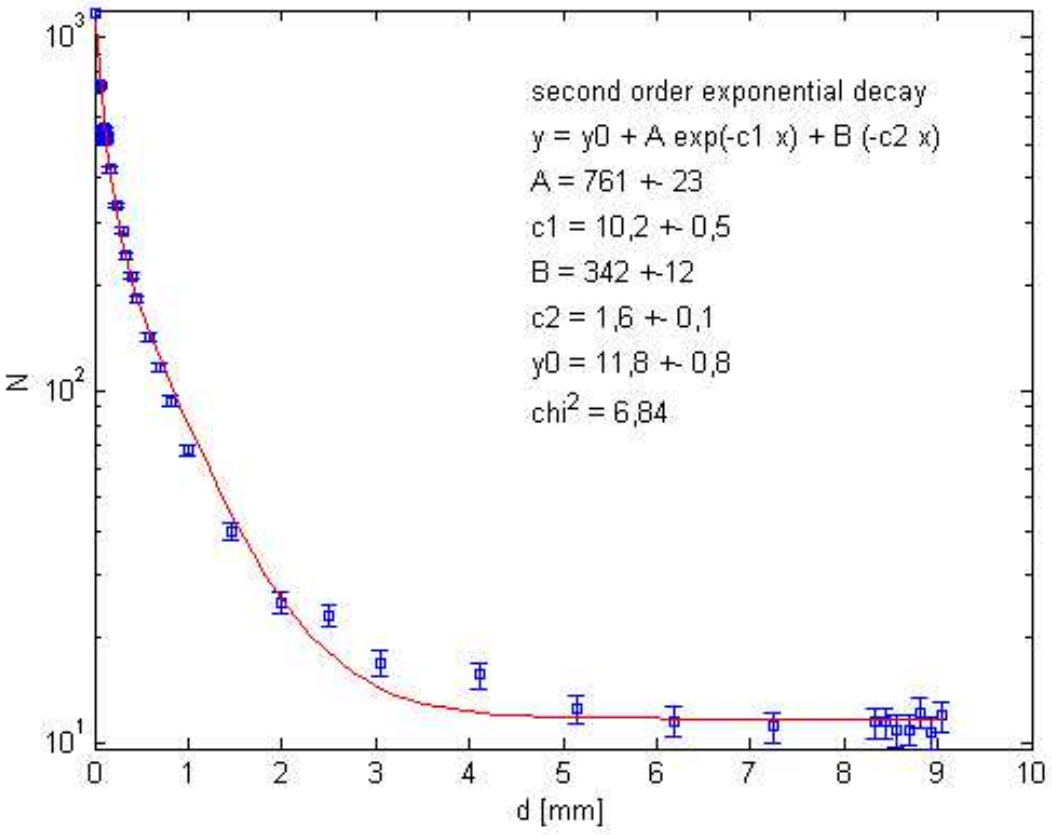

Figure 8: Logarithmic plot of the exponential decrease.

6 Error analysis

6.1 Statistics

The statistic distributions are assumed to be Poisson distributions. All counts, except for the histogram, were performed at 10s intervalls, which gives an error of

$$\Delta z = \sqrt{\frac{z}{10}} \approx \frac{1}{3}\sqrt{z}$$

6.2 Dead time of the counter

We assume that our measurement was correct up to 0.2 scale divisions, so the estimated error is $\pm\, 4\mu$s.

6.3 β radiation energy distribution

6.3.1 Teslameter

According to the manual, the teslameter has an error of 2% of reading.

6.3.2 Error for the radius r

We made certain, that our geometry is as accurate as possible, so we assume no measuring method error on r = 3.39cm. However both the counter and the source are not point objects, so particles can have trajectories with radii other than r, see fig. 9. This results in errors when using the fixed radius r. The error on the radius can be graphically estimated by the difference between the ideal radius and the radius with the largest deviation from the ideal radius, as shown in fig.9.
This worst-case estimate will produce an unnecessary large error, therefore the estimation parameters have been altered to get a more realistic estimate.

Let Ω and Ξ be two concentric circles with the radii R_Ω and R_Ξ. R_Ξ is a constant, R_Ω is random.
Assume that R^* is a value between R_Ξ and 0. We are interested in the probability that R_Ω is smaller than R^*. The probability density is

$$p\left(R^*\right) = \frac{1}{R_\Xi}\,\Theta(0 \leq R^* \leq R_\Xi)$$

The probabilty for R_Ω being smaller than R^* is given by the integral

$$P\left(R_\Omega \leq R^*\right) = \int_0^{R^*} dR^{*'}\, p(R^{*'}) = \frac{R^*}{R_\Xi}$$

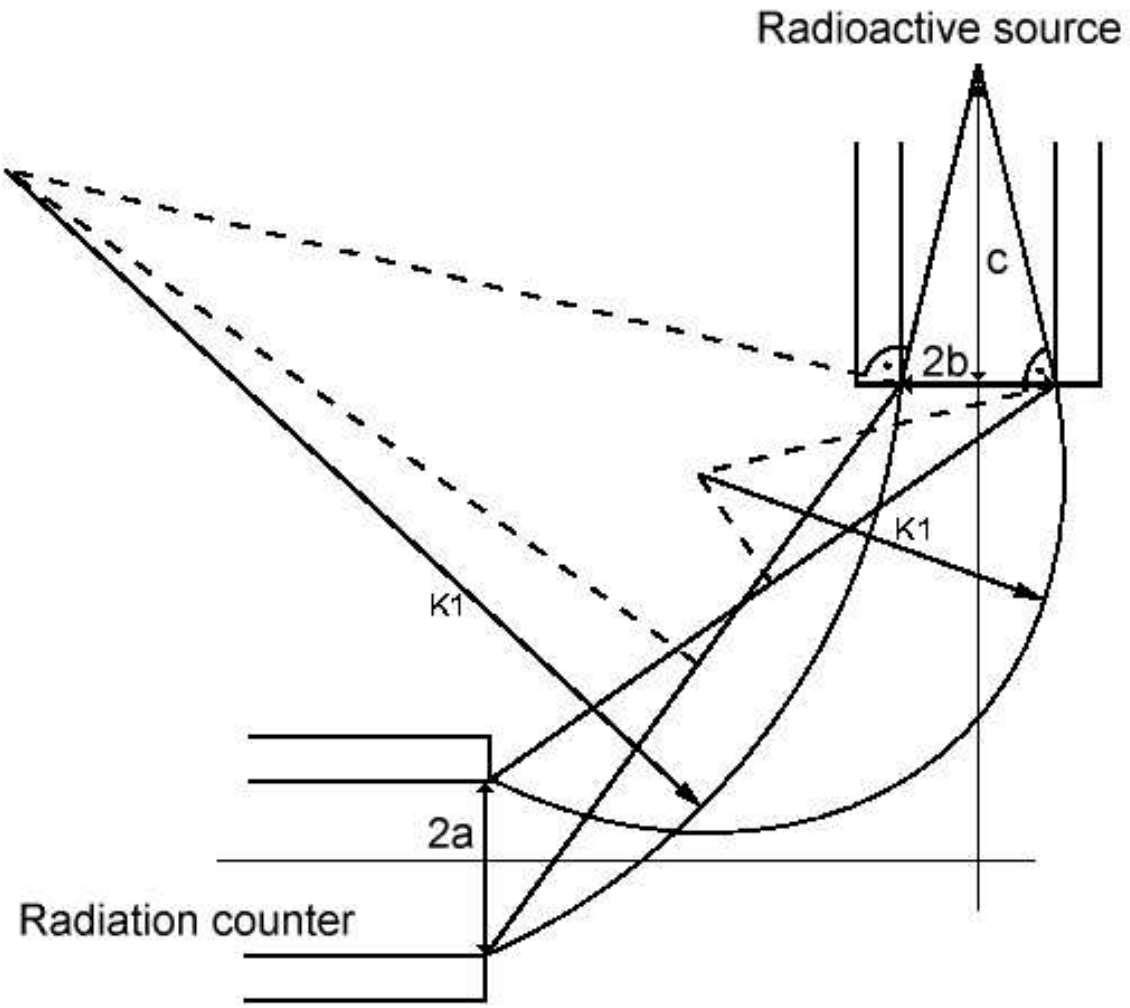

Figure 9: Different possible radii.

This allows us to determine R* for $\mathrm{P}\left(R_\Omega \leq R^*\right) = 1 - \frac{1}{e}$.

We associate R_Ξ with the radii of the collimator hole resp. the counter window, R_Ω with the point where the trajectory of a particle intersects the collimator hole resp. the counter window. We calculate the radius of the circular areas through which 63% of the particles travel and make a graphical estimate according to fig.9, using the obtained dimensions for 63% of the particles. These are:

$$2a = 0,63 \cdot 9mm = 5,7mm$$

$$2b = 0,63 \cdot 5mm = 3,2mm$$

The graphical estimate gives gives $r = (3,4 \pm 0,6)\,cm$.

$$\frac{\Delta r}{r} \approx 0,18$$

6.3.3 Particle energy

The errors for B and r allow us to specify errors for the velocity and the energy of the particles, which are shown in fig.6. Compared to the error on r, the error on B is small and will be neglected.

$$\Delta E = |\frac{\partial E}{\partial r}|\Delta r$$

$$\frac{\partial E}{\partial r} = \frac{p^2}{Er}$$

The error for the maximum energy was calculated from the error of the straight line at the intersection with the x-axis given by Matlab.

$$\Delta E = \frac{\Delta f(z)}{k}$$

where f(z) is $\frac{\sqrt{z}}{\sqrt{p^3\,F(Z',E)}}$ and k is the slope of the straight line.

6.4 Absorption of radiation in aluminium

The error on the absorption coefficients is given by the fit routine of Origin and was used as specified by Origin. For subtracting the background radiation, we took the value from the energy distribution measurement. However in this measurement, the distance between the two magnetic cores was ≈8mm, which is about 10% smaller than the diameter of the counter window. Therefor the actual background radiation is presumably slightly larger, but we consider this neglectable.

7 Summary

7.1 Statistic distribution of the count rate

A Poisson distribution was observed which was approximated by a Gauss distribution, see fig.4. This is reasonable because the approximation is already good at values of one order of magnitude lower than the measured values[5].

7.2 Characteristic curve of the radiation counter

The characteristic curve is shown in fig.5. A linear fit was performed to calculate the slope of the plateau, which is approximately

$$k = -11 \frac{\%}{100\,V}$$

7.3 Dead time of the radiation counter

The dead times for various voltages are shown in table 5.2. For our measurements we operated the radiation counter at 500 V with a dead time of $(140 \pm 4)\mu$s.

7.4 Energy distribution and maximum energy of β particles

The energy distribution is shown in fig.6 and as Kurie plot in fig.7. The maximum energy of the β particles was $E_{max} = (3127 \pm 133)keV$, which is the energy of a particle moving at $\approx 99\%$ of the speed of light.

7.5 Absorption of radiation in aluminium

A second order exponential decrease fit was done to calculate the absorption coefficients for the two dominant radiating materials. The coefficients are

$$c_1 = (16 \pm 1)mm^{-1}$$

$$c_2 = (2,5 \pm 0,2)mm^{-1}$$

The second order exponential decrease is shown in fig.8.

[5] see appendix.

8 Appendix

8.1 Radium decay series

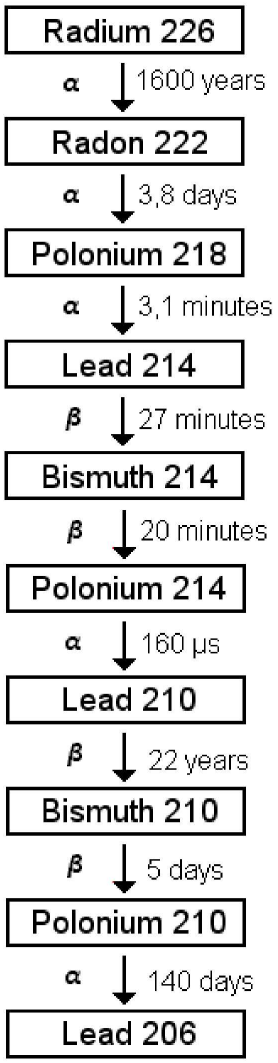

Figure 10: Decay series for the three Radium isotopes.

8.2 Gauss and Poisson distribution

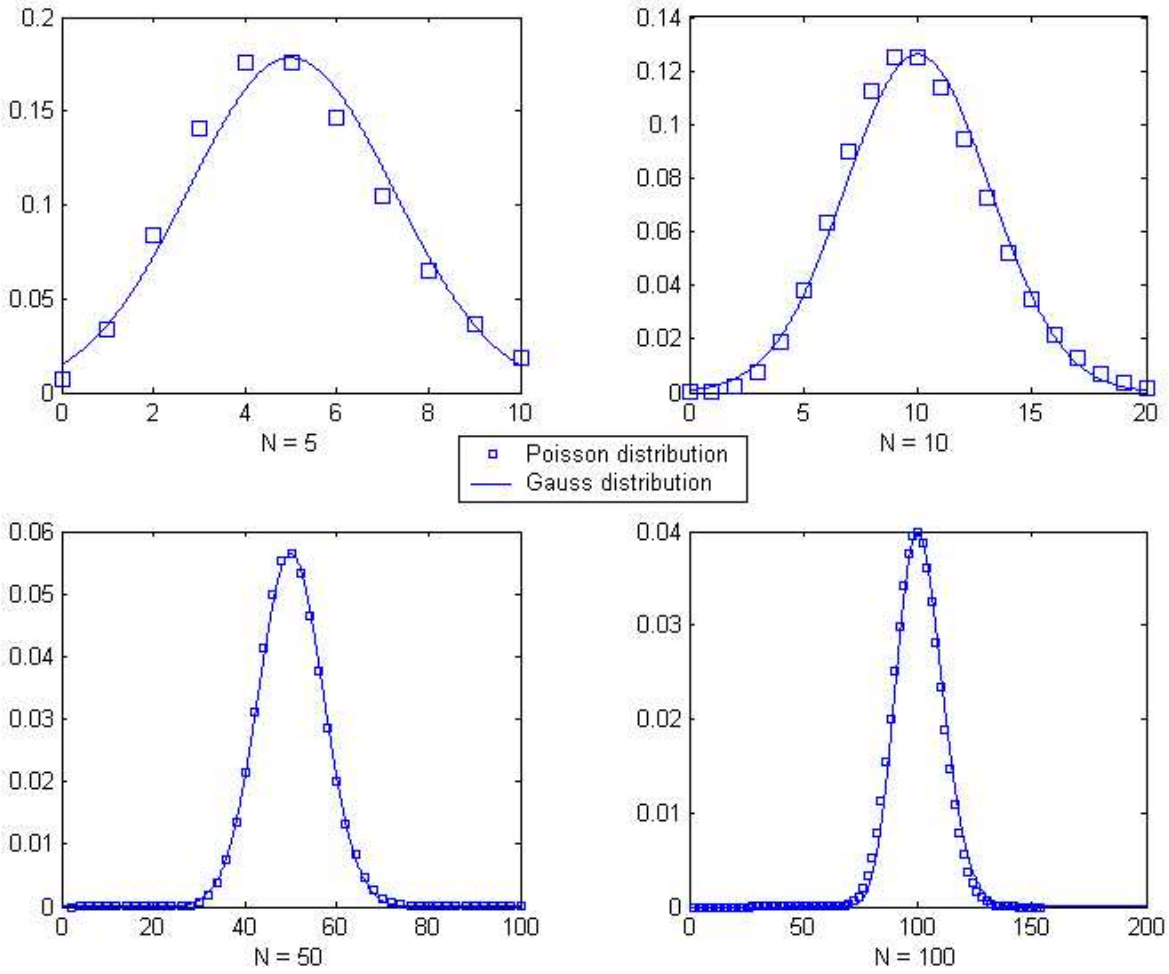

Figure 11: Comparison of Gauss and Poisson distribution.

Gauss distribution with $\sigma \approx \sqrt{N}$:

$$P(X|N) = \frac{1}{\sqrt{2\pi N}} e^{-\frac{(x-N)^2}{2N}}$$

Poisson distribution:

$$P(X|N) = \frac{N^x}{x!} e^{-N}$$

For large N, the factorial was approximated with the Stirling formula

$$x! \approx x^{x+\frac{1}{2}} e^{-x} \sqrt{2\pi}$$